Structural phase transitions in the ferroelectric oxides $Ba_{1-x}Pb_xBi_2Nb_2O_9$ (x = 0.375,0.625)

2004 J. Phys.: Condens. Matter 16 5443

(http://iopscience.iop.org/0953-8984/16/30/007)

INSTITUTE OF PHYSICS PUBLISHING JOURNAL OF PHYSICS: CONDENSED MATTER

J. Phys.: Condens. Matter **16** (2004) 5443–5452 PII: S0953-8984(04)80269-8

Structural phase transitions in the ferroelectric oxides $Ba_{1-x}Pb_xBi_2Nb_2O_9$ ($x = 0.375, 0.625$)

Rene Macquart[1], **Brendan J Kennedy**[1], **Takashi Kamiyama**[2] **and Fujio Izumi**[3]

[1] The Centre for Heavy Metals Research, School of Chemistry, The University of Sydney, New South Wales 2006, Australia
[2] Neutron Science Laboratory, Institute of Materials Structure Science, High Energy Accelerator Research Organization, 1-1, Oho, Tsukuba, Ibaraki 305-0801, Japan
[3] Advanced Materials Laboratory, National Institute for Materials Science, 1-1 Namiki, Tsukuba, Ibaraki 305-0044, Japan

Received 5 May 2004
Published 16 July 2004
Online at stacks.iop.org/JPhysCM/16/5443
doi:10.1088/0953-8984/16/30/007

Abstract

Temperature induced structural phase transitions in the lead doped Aurivillius oxides $Ba_{1-x}Pb_xBi_2Nb_2O_9$ ($x = 0.375, 0.625$) are explored using powder neutron diffraction methods in the context of the pure parent compounds, $PbBi_2Nb_2O_9$ and $BaBi_2Nb_2O_9$. At both lead concentrations the system is found to exhibit behaviour similar to that found in $PbBi_2Nb_2O_9$. That is, at room temperature the oxides are orthorhombic and the Pb rich compound transforms to a tetragonal structure via a second orthorhombic form. The presence of Ba lowers the phase transition temperatures relative to the undoped lead compound but is not sufficient to induce a change in the general mode of structural transition.

(Some figures in this article are in colour only in the electronic version)

1. Introduction

The recent interest in ferroelectric materials in terms of their suitability for incorporation into non-volatile random access memory technologies has led to a number of studies on $SrBi_2Ta_2O_9$ [1–3]. Related compounds of the type $ABi_2M_2O_9$ (A = Ca, Sr, Ba, Pb; M = Nb, Ta) have undergone similar scrutiny [4–7]. These compounds apparently display two general phase transition pathways, typified by $PbBi_2Nb_2O_9$ (PBN) and $BaBi_2Nb_2O_9$ (BBN). While $PbBi_2Nb_2O_9$ and $BaBi_2Nb_2O_9$ are structurally similar at high temperatures, sharing the same space group ($I4/mmm$), the onset of ferroelectricity at lower temperatures is achieved by two distinctly different paths. $PbBi_2Nb_2O_9$ follows the same behaviour as $SrBi_2Ta_2O_9$, transforming continuously from space group $I4/mmm$ to $A2_1am$ via an intermediate

orthorhombic phase *Amam* [8]. The existence of an intermediate phase was postulated from first-principles electronic structure calculations by Stachiotti *et al* [9]. Termed a displacive ferroelectric, spontaneous polarization occurs along the *a* axis as a result of the combination of octahedral tilt and cation displacement. Both the high temperature, *Amam* and $I4/mmm$, phases are paraelectric, whereas the structure in space group $A2_1am$ may be ferroelectric. In contrast, $BaBi_2Nb_2O_9$ has historically been classed as a relaxor type ferroelectric although somewhat different from conventional relaxors such as $PbMg_{1/3}Nb_{2/3}O_3$ [10]. It has been assumed that BBN remained in the tetragonal space group $I4/mmm$ even after the onset of ferroelectric behaviour and it was suggested that the ferroelectricity was a result of orthorhombic microdomains with the exceptionally broad ferroelectric transition a result of cation disorder between the perovskite and Bi layers [6, 11]. Shimakawa *et al* [12] presented similar conclusions for the isostructural $BaBi_2Ta_2O_9$. We have recently found evidence for a structural phase transition in BBN [13] near the Curie temperature and using a combination of high resolution neutron and synchrotron diffraction methods together with group theory suggested that this could be due to a transition from the high temperature tetragonal paraelectric phase in space group $I4/mmm$ to a low temperature tetragonal ferroelectric phase in space group $I4mm$. Cation disorder in both phases still plays an essential role in broadening the ferroelectric transition.

Doping of layered perovskites is commonly used to enhance their favourable ferroelectric properties [14], although the origins of the altered performance are often unclear [15, 16]. Substituting increasingly more Sr into $Ba_{1-x}Sr_xBi_2Nb_2O_9$ solid solutions decreases the broadness of the ferroelectric transition, the resulting compounds behaving more and more like pure $SrBi_2Nb_2O_9$ [11]. The work presented here investigates the substitution of Pb onto the Ba site in $BaBi_2Nb_2O_9$ to form solid solutions of the type $Ba_{1-x}Pb_xBi_2Nb_2O_9$ in order to examine the phase transition behaviour across the Curie temperature, the aim being to determine the influence of Pb on the ferroelectric to paraelectric phase transition.

2. Experimental details

Samples of $Ba_{0.375}Pb_{0.625}Bi_2Nb_2O_9$ and $Ba_{0.625}Pb_{0.375}Bi_2Nb_2O_9$ were synthesized using standard solid state synthetic techniques. In each case a stoichiometric mixture of high purity (>99%) $BaCO_3$, PbO, Bi_2O_3 and Nb_2O_5 was ground in acetone then placed in open alumina crucibles and heated for 15 h at 700 °C, 65 h at 850 °C, 65 h at 900 °C, 65 h at 950 °C, 48 h at 1000 °C, 24 and 48 h at 1050 °C, then 48 h at 1100 °C, the material being reground between each heating step. The somewhat long preparation does not necessarily represent an optimized route for the synthesis of these compounds, merely the most expedient route employed at the time with particular care being taken to minimize the loss of the more volatile Pb. Neutron diffraction experiments were carried out using the high resolution powder diffractometer SIRIUS at KENS [17]. Time of flight constants DIFC = 15 436.89 and DIFA = −11.48 were established during the measurements. High temperature data were collected with the aid of a custom built Miller type furnace while the low temperature data were collected using a closed cycle cryostat. Diffraction patterns were collected from 20 to 600 °C in ∼25 °C steps using the 90° detector bank for $Ba_{0.375}Pb_{0.625}Bi_2Nb_2O_9$. Owing to restrictions on beam time, data were only collected at 20 and 300 K for $Ba_{0.625}Pb_{0.375}Bi_2Nb_2O_9$. All Rietveld refinements were carried out using Rietica [18].

3. Results

From the previous work on $PbBi_2Nb_2O_9$ and $BaBi_2Nb_2O_9$ conducted by the authors [13, 19] it seemed likely that $Ba_{0.375}Pb_{0.625}Bi_2Nb_2O_9$ and $Ba_{0.625}Pb_{0.375}Bi_2Nb_2O_9$ would display

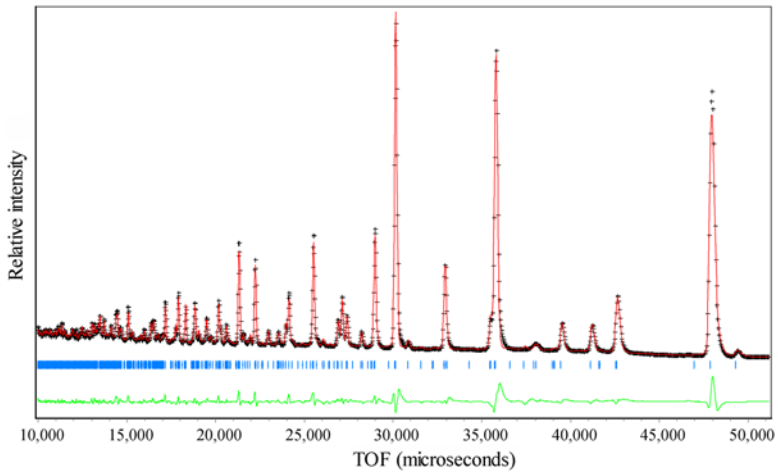

Figure 1. Neutron powder diffraction pattern for $Ba_{0.375}Pb_{0.625}Bi_2Nb_2O_9$ at 25 °C. The line at the bottom shows the difference between the observed (crosses) and the calculated pattern (line) while the vertical bars show the Bragg reflection positions corresponding to the model.

behaviour similar to one of the two parent compounds (PBN or BBN) in terms of adopting one or the other of their established phase transition mechanisms. The structure of $Ba_{0.375}Pb_{0.625}Bi_2Nb_2O_9$ was initially refined in space group $A2_1am$ from 20 to 600 °C, this being a sensible starting point since $PbBi_2Nb_2O_9$ adopts a structure in this space group below 575 °C. Figure 1 shows a typical neutron diffraction pattern. While there are no obvious signs of orthorhombic splitting, careful examination of the neutron diffraction plots revealed additional weak 'superlattice' peaks characteristic of orthorhombic symmetry, figure 2. The loss of these peaks and convergence of the a and b lattice parameters indicated that the compound became tetragonal at 500 °C, figure 3. The degree of orthorhombicity at 20 °C is 0.14%. A change in slope of the thermal expansion curves for all three lattice parameters at 275 °C suggested a phase transition. Using the computer program ISOTROPY [20] a paraelectric intermediate phase in space group $Amam$ was identified. Subsequent refinements in space group $Amam$ in the region between 275 and 500 °C yielded fits similar to the $A2_1am$ model. The small anomaly in the plot near 100 °C is most likely due to a change in the heating conditions at this temperature. The high temperature phase refines well in space group $I4/mmm$ and the low temperature phase is well fitted in space group $A2_1am$ while the intermediate phase refined well in space group $Amam$, table 1. The room temperature data collected at 20 °C gave a good fit in the orthorhombic space group $A2_1am$ and did not differ significantly from those collected at 100 °C, listed in table 2. It is concluded that the phase transition sequence is $A2_1am$–$Amam$–$I4/mmm$ in agreement with that observed for the structurally related Ta oxides $SrBi_2Ta_2O_9$ and $Sr_{0.85}Bi_{2.1}Ta_2O_9$ [8, 21]. The nature of these transitions is apparently consistent with the first principles calculations [9].

The first phase transition temperature of ∼275 °C is located above that of BBN but below the Curie temperature of PBN (560 °C) [22] with the transition to space group $I4/mmm$ occurring some 200 °C below that found for PBN (700 °C). It appears that the addition of a small amount of Ba to PBN serves to decrease the Curie temperature while leaving the sequence of phase transitions unchanged from that seen in the undoped Pb compound. In the absence of suitable synchrotron x-ray measurements the extent of cation disorder between the $[Bi_2O_2]^{2+}$ layer and the perovskite layer could not be accurately modelled but it seems likely that the Ba^{2+} ions (ionic radius 1.61 Å) substitute onto the site of the smaller Pb^{2+} ions (ionic radius

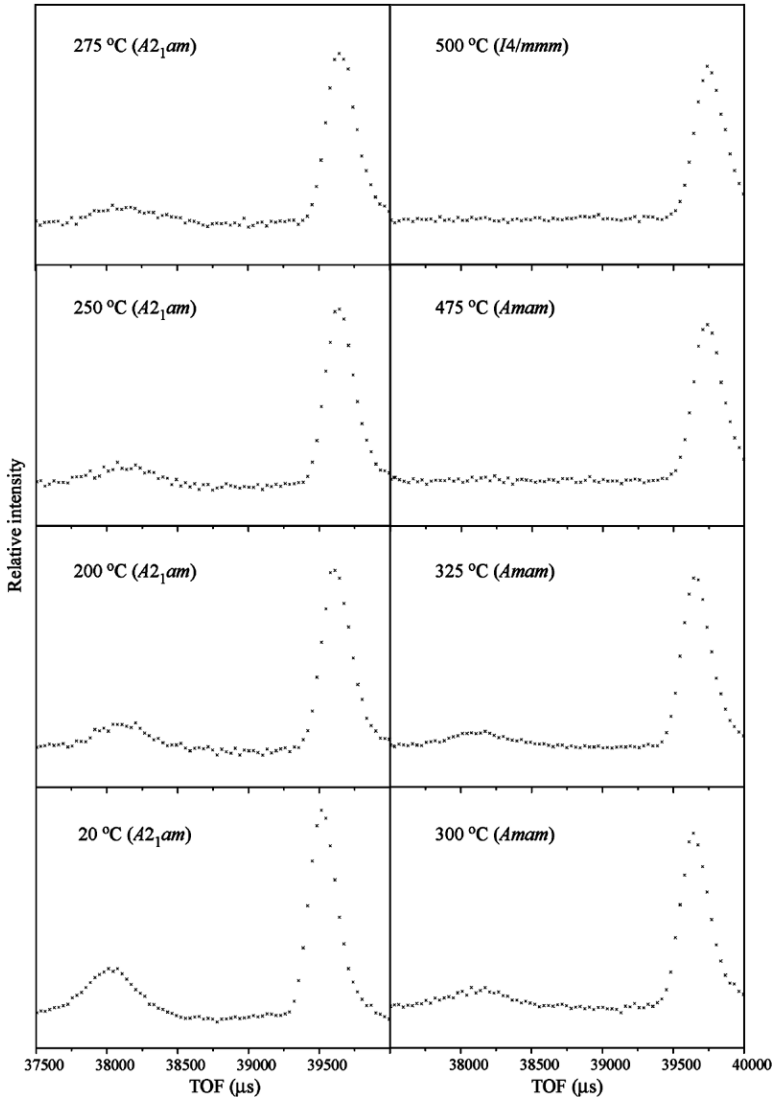

Figure 2. Portions of the observed neutron powder diffraction patterns for $Ba_{0.375}Pb_{0.625}Bi_2Nb_2O_9$. The (211) and (120) reflections near 38 000 μs ($d = 2.46$ Å) are a convenient indicator of orthorhombic symmetry.

1.49 Å), thereby reducing the octahedral NbO_6 tilting (O2–O1–O2 tilt angle: $A2_1am$, PBN 9.6°, $Ba_{0.375}Pb_{0.625}$ 4.7°; $Amam$, PBN 9.2°, $Ba_{0.375}Pb_{0.625}$ 0.6°), which in turn lowers both the $A2_1am$ to $Amam$ and the $Amam$ to $I4/mmm$ phase transition temperatures compared to pure PBN.

The tilting in the perovskite double layer acts to reduce the strain on the system as the undersized Ba and Pb cations are substituted into the cavities between NbO_6 octahedra. Figure 4 shows how the NbO_6 octahedra tilt away from the higher symmetry tetragonal parent structure ($I4/mmm$) as the temperature is varied. A non-zero O2–O1–O2 tilt angle indicates a movement away from a perfect alignment of the octahedra. At room temperature it can be seen that the octahedra are considerably tilted. As the temperature is raised the tilting

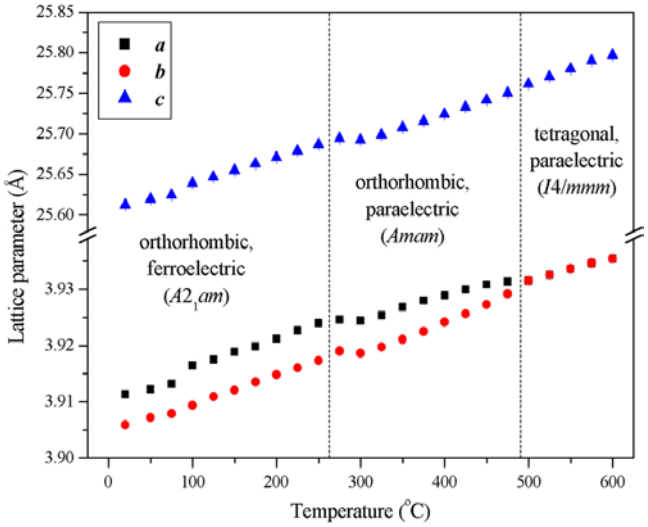

Figure 3. The temperature dependence of lattice parameters of $Ba_{0.375}Pb_{0.625}Bi_2Nb_2O_9$. The orthorhombic values have been divided by $\sqrt{2}$ to make them comparable to the tetragonal values.

Table 1. Refined lattice parameters and measures of fit for $Ba_{0.375}Pb_{0.625}Bi_2Nb_2O_9$. (Note: The orthorhombic lattice parameters have been referenced to a tetragonal cell ($a/\sqrt{2}$, $b/\sqrt{2}$) for the sake of comparison.)

Temp. (°C)	Space group	a (Å)	b (Å)	c (Å)	R_p (%)	R_{wp} (%)
20	$A2_1am$	3.911 4(3)	3.905 9(3)	25.611 9(7)	4.99	7.25
50	$A2_1am$	3.912 2(4)	3.907 2(4)	25.619 2(8)	5.18	7.45
75	$A2_1am$	3.913 1(3)	3.907 9(3)	25.624 2(7)	4.86	7.09
100	$A2_1am$	3.916 4(3)	3.909 4(3)	25.638 9(8)	5.54	8.34
125	$A2_1am$	3.917 5(3)	3.910 9(3)	25.646 5(9)	5.70	8.72
150	$A2_1am$	3.918 8(3)	3.912 1(3)	25.654 5(8)	5.51	8.36
175	$A2_1am$	3.919 9(3)	3.913 5(3)	25.662 9(8)	5.17	7.85
200	$A2_1am$	3.921 2(3)	3.914 8(3)	25.670 6(8)	5.04	7.74
225	$A2_1am$	3.922 7(3)	3.916 0(3)	25.678 5(9)	5.59	8.52
250	$A2_1am$	3.924 0(3)	3.917 3(3)	25.686 4(8)	5.17	7.90
275	$Amam$	3.924 6(3)	3.919 0(3)	25.694 02(8)	4.79	7.46
300	$Amam$	3.924 4(3)	3.918 6(3)	25.692 1(8)	4.67	7.36
325	$Amam$	3.925 4(3)	3.919 8(3)	25.698 46(7)	4.37	7.02
350	$Amam$	3.926 9(3)	3.921 1(3)	25.707 27(7)	4.56	7.10
375	$Amam$	3.928 0(3)	3.922 5(3)	25.715 06(8)	4.48	7.07
400	$Amam$	3.928 9(3)	3.924 2(3)	25.723 76(7)	4.33	6.75
425	$Amam$	3.929 9(3)	3.925 7(3)	25.732 5(7)	4.23	6.59
450	$Amam$	3.930 9(3)	3.927 3(4)	25.741 19(7)	4.17	6.55
475	$Amam$	3.931 3(5)	3.929 2(5)	25.749 94(7)	4.18	6.55
500	$I4/mmm$	3.931 55(6)	3.931 55(6)	25.761 09(8)	4.16	6.54
525	$I4/mmm$	3.932 56(5)	3.932 56(5)	25.769 97(7)	4.16	6.51
550	$I4/mmm$	3.933 65(5)	3.933 65(5)	25.779 76(7)	4.15	6.48
575	$I4/mmm$	3.934 68(5)	3.934 68(5)	25.789 91(7)	4.16	6.50
600	$I4/mmm$	3.935 42(5)	3.935 42(5)	25.796 87(7)	3.81	6.23

remains essentially the same, within the limits of the error, until at 275 °C the phase change to *Amam* results in a substantial decrease in the octahedral tilt angles. As the temperature is

Table 2. Atomic coordinates of $Ba_{0.375}Pb_{0.625}Bi_2Nb_2O_9$ at various temperatures from neutron data.

Atom	*Wykoff*	*x*	*y*	*z*	B_{iso} (Å^2)
			100 °C ($A2_1am$)		
Ba	4a	3/4[a]	0.768(3)	0	2.8(2)
Pb	4a	3/4[a]	0.768(3)	0	2.8(2)
Bi	8b	0.742(6)	0.748(1)	0.2017(2)	2.01(9)
Nb	8b	0.737(6)	0.757(2)	0.5887(1)	0.43(6)
O1	4a	0.720(8)	0.297(3)	0	2.2(3)
O2	8b	0.742(7)	0.743(4)	0.6590(2)	2.7(2)
O3	8b	0.995(6)	0.019(9)	0.2497(8)	1.6(2)
O4	8b	0.994(5)	0.988(6)	0.0763(5)	1.8(3)
O5	8b	0.023(5)	0.952(4)	0.4193(6)	2.1(4)
			400 °C ($Amam$)		
Ba	4c	3/4[a]	0.760(4)	0	3.6(1)
Pb	4c	3/4[a]	0.760(4)	0	3.6(1)
Bi	8g	3/4	0.747(2)	0.2019(1)	2.48(8)
Nb	8g	3/4	0.746(2)	0.5886(1)	0.61(5)
O1	4c	3/4	0.282(4)	0	2.8(2)
O2	8g	3/4	0.774(4)	0.6584(2)	2.9(2)
O3	8e	0	0	0.2510(8)	1.7(1)
O4	8e	0	0	0.0805(6)	3.0(4)
O5	8e	0	0	0.4235(6)	2.5(3)
			600 °C ($I4/mmm$)		
Ba	2b	0	0	1/2	4.0(1)
Pb	2b	0	0	1/2	4.0(1)
Bi	4e	0	0	0.7019(1)	2.97(8)
Nb	4e	0	0	0.0885(1)	0.77(5)
O1	2a	0	0	0	3.5(2)
O2	4e	0	0	0.1580(2)	3.9(1)
O3	4d	0	1/2	1/4	1.9(1)
O4	8g	0	1/2	0.0785(1)	2.87(8)

[a] Atomic coordinates fixed in order to define the polar axis in $A2_1am$. In $Amam$ this site occupies a special position.

further increased the tilt angles decrease slowly until the structure becomes tetragonal with the NbO_6 octahedra perfectly aligned at 500 °C and above. Unfortunately, the temperature intervals are too coarse to establish if the temperature dependence of the reduction in tilt is consistent with a first order or continuous phase transition. Group theory and the temperature dependence of the lattice parameters suggest the transition will be continuous, whereas the temperature dependence of the tilt is indicative of a first order $A2_1am$ to $Amam$ transition. It would be very informative to study the transition at still finer temperature intervals. At low temperatures the structure is in space group $A2_1am$ wherein the octahedra can tilt about two axes (figure 5). Moving to the higher symmetry $Amam$ the octahedra are restricted to one axis of tilt, while at high temperatures $Ba_{0.375}Pb_{0.625}Bi_2Nb_2O_9$ adopts a structure in space group $I4/mmm$, removing the remaining tilt axis. There is no reason to doubt that the $Amam$ to $I4/mmm$ transition in $Ba_{0.375}Pb_{0.625}Bi_2Nb_2O_9$ is continuous.

Representative atomic coordinates for the three phases are listed in table 2. In the absence of comparable x-ray diffraction data it was not practical to refine the disorder between the

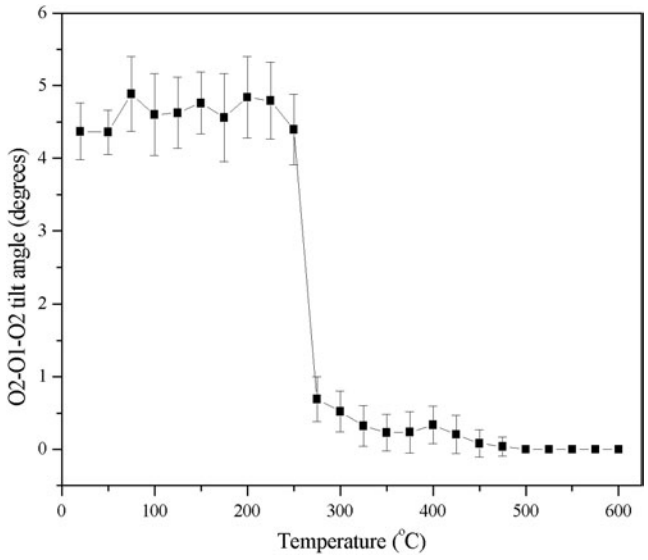

Figure 4. Octahedral tilting in $Ba_{0.375}Pb_{0.625}Bi_2Nb_2O_9$ as a function of temperature. The bars indicate the standard deviation in the angle.

Ba/Pb and Nb cations and an ideal distribution has been assumed. The atomic coordinates and displacement parameters for the cations on the same crystallographic sites have been constrained to be equal. The displacement parameters for the disordered Pb/Ba cations in each phase are slightly higher than those of the Nb and O ions and this possibly reflects some disordering of these onto the Bi site. The displacement parameters of the various atoms, in particular, increase slightly as the temperature is increased, which is a normal consequence of heating the sample.

It is concluded that the Pb rich $Ba_{0.375}Pb_{0.625}Bi_2Nb_2O_9$ adopts a similar phase transition behaviour to that observed in $PbBi_2Nb_2O_9$, namely

$$\underset{\text{ferroelectric}}{A2_1am} \xrightarrow{275\,^\circ\text{C}} \underset{\text{paraelectric}}{Amam} \xrightarrow{500\,^\circ\text{C}} \underset{\text{paraelectric}}{I4/mmm}.$$

Powder x-ray diffraction measurements of $Ba_{0.625}Pb_{0.375}Bi_2Nb_2O_9$ suggest that this is tetragonal at room temperature. The powder neutron diffraction data at both 20 and 300 K, however, revealed the presence of weak (211) and (120) reflections indicative of orthorhombic symmetry at both temperatures (figure 6). This highlights a major limitation of x-ray diffraction methods in the study of oxides where the distortion from the metric may be sufficiently small so as not to result in measurable splitting of the reflections. The refined atomic coordinates and lattice parameters obtained by Rietveld refinements from these data are listed in table 3. The low temperature data are best fitted to a model in space group $A2_1am$ while the 300 K data fit similarly well in space groups $I4/mmm$ and $A2_1am$ (table 4), with a slight preference for $A2_1am$. The observation of superlattice reflections, indicative of NbO_6 tilting, demonstrates more definitively that the structure is orthorhombic. Reliance on the R-factors is not sufficient to distinguish between the possible structures, especially considering the large difference in the number of variable parameters in the orthorhombic and tetragonal models.

The tilt angle in $Ba_{0.625}Pb_{0.375}Bi_2Nb_2O_9$ at room temperature is 1.0(7)°, which is reduced from that seen in the $A2_1am$ phase of $Ba_{0.375}Pb_{0.625}Bi_2Nb_2O_9$. The tilting of the NbO_6 octahedra in the orthorhombic phases can be viewed as arising from a mismatch between the bonding requirements of the Nb and Ba/Pb cations in the ABO_3 type perovskite layers.

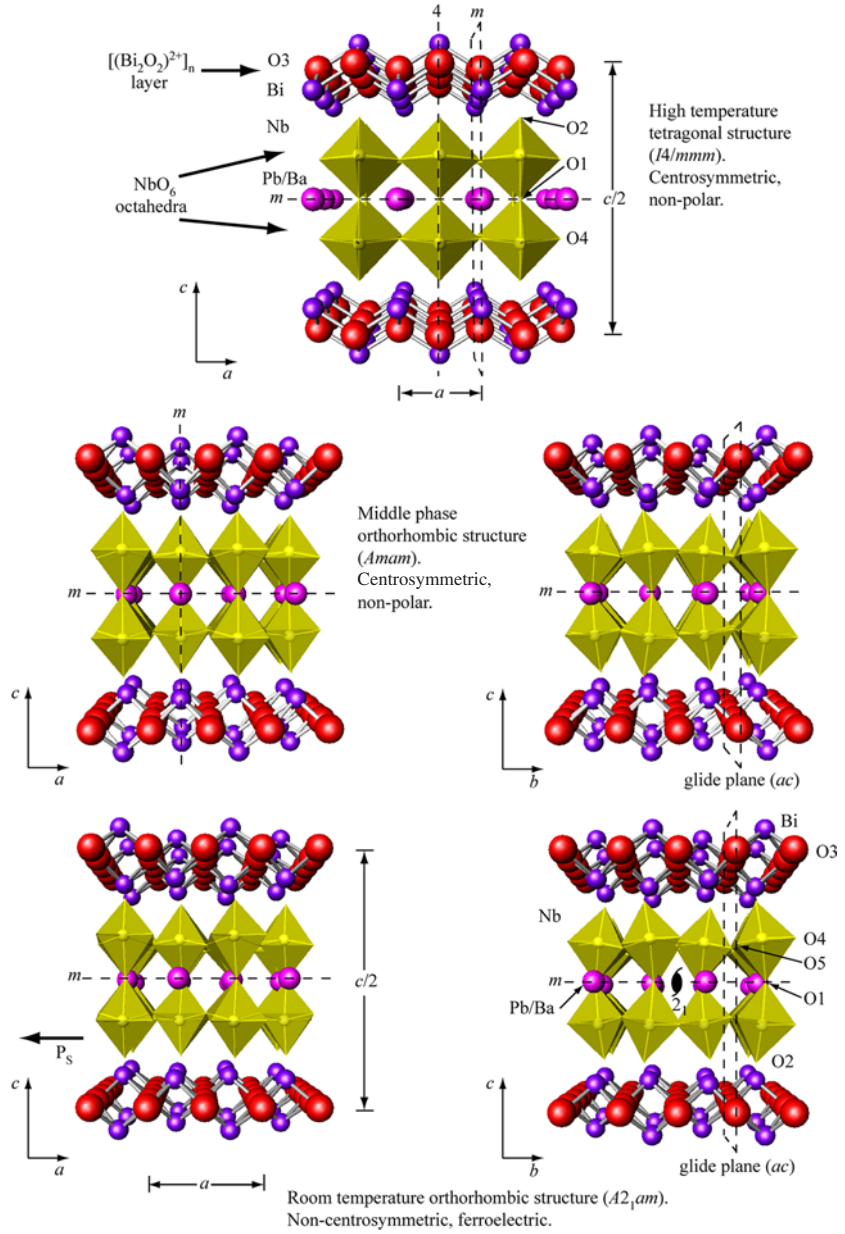

Figure 5. The structure of $Ba_{1-x}Pb_xBi_2Ta_2O_9$ ($x = 0.375, 0.625$) at various temperatures showing key mirror planes (m), glide planes and rotation and screw axes (4, 2_1). Note the change in the direction of the axes in this figure.

This can be quantified by the tolerance factor, t, defined as $t = \frac{r_{A-O}}{\sqrt{2}r_{B-O}}$ where r_{A-O} and r_{B-O} represent the ideal A–O and B–O bond lengths respectively as given by the sum of the appropriate ionic radii. Partially replacing Ba^{2+} with the smaller Pb^{2+} cation increases the value of t and hence reduces the magnitude of the NbO_6 tilts.

The a and b lattice parameters for $Ba_{0.625}Pb_{0.375}Bi_2Nb_2O_9$ at 300 K are very similar, indicating that the structure might be approaching transition to a tetragonal form, the

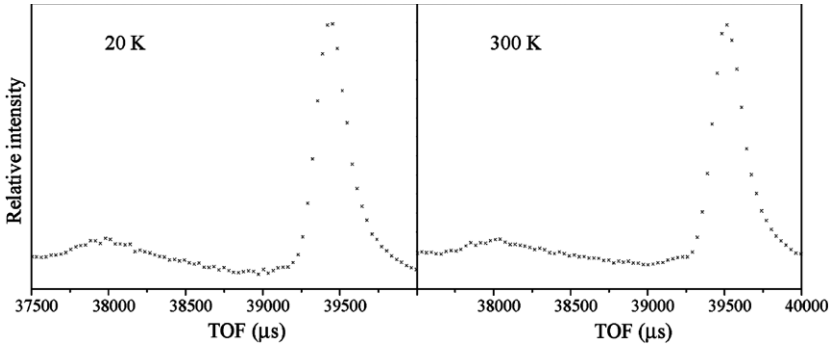

Figure 6. Portions of the observed neutron powder diffraction patterns for $Ba_{0.625}Pb_{0.375}Bi_2Nb_2O_9$. The (211) and (120) reflections near 38 000 μs ($d = 2.46$ Å) were used to detect the orthorhombic phases.

Table 3. Atomic coordinates of $Ba_{0.625}Pb_{0.375}Bi_2Nb_2O_9$ at 20 and 300 K.

Atom	x	y	z	B_{iso} (Å^2)
		20 K ($A2_1am$)		
Ba	3/4[a]	0.737(4)	0	0.9(2)
Pb	3/4[a]	0.737(4)	0	0.9(2)
Bi	0.724(4)	0.750(2)	0.2026(1)	1.70(8)
Nb	0.724(5)	0.754(2)	0.5883(1)	0.37(6)
O1	0.732(7)	0.218(4)	0	2.3(3)
O2	0.726(5)	0.729(3)	0.6602(2)	1.6(1)
O3	0.981(4)	0.98(2)	0.248(1)	1.2(1)
O4	0.000(5)	0.036(6)	0.079(1)	0.8(5)
O5	0.980(5)	0.000(6)	0.422(1)	2.4(5)
		300 K ($A2_1am$)		
Ba	3/4[a]	0.737(4)	0	1.3(2)
Pb	3/4[a]	0.737(4)	0	1.3(2)
Bi	0.723(5)	0.752(2)	0.2026(1)	2.29(9)
Nb	0.722(6)	0.756(2)	0.5884(1)	0.58(7)
O1	0.732(8)	0.213(4)	0	2.8(3)
O2	0.727(6)	0.722(3)	0.6598(2)	2.0(2)
O3	0.982(5)	0.00(2)	0.2484(8)	1.0(1)
O4	0.994(6)	0.033(5)	0.0775(6)	1.7(3)
O5	0.984(6)	0.004(6)	0.4204(7)	2.1(4)

[a] Atomic coordinates fixed in order to define polar axis in $A2_1am$.

Table 4. Lattice parameters and quality of fit for $Ba_{0.625}Pb_{0.375}Bi_2Nb_2O_9$ at 20 and 300 K.

Temp. (K)	Space group	a (Å)	b (Å)	c (Å)	R_p	R_{wp}
20	$A2_1am$	5.542 0(3)	5.530 5(3)	25.557 9(8)	6.12	7.67
300	$A2_1am$	5.546 11(9)	5.545 81(9)	25.608 7(8)	4.76	6.25
300	$Amam$	5.546 1(2)	5.545 801(8)	25.608 2(8)	4.92	6.51
300	$I4/mmm$	3.921 52(6)	3.921 52(6)	25.609 3(7)	4.81	6.70

orthorhombic distortion at room temperature being 0.005%. 300 K is well below the literature Curie temperatures of either BBN (473 K) or PBN (833 K) [22], suggesting that $Ba_{0.625}Pb_{0.375}Bi_2Nb_2O_9$ is actually still ferroelectric and hence belongs in space group $A2_1am$.

It is possible that $Ba_{0.625}Pb_{0.375}Bi_2Nb_2O_9$ will become metrically tetragonal below the Curie temperature while still remaining in space group $A2_1am$ as was found for $PbBi_2Ta_2O_9$ [19]. Further variable temperature neutron and synchrotron diffraction experiments on this and related compositions are required in order to provide a clearer picture.

4. Conclusion

Variable temperature powder neutron diffraction measurements have demonstrated that the mixed Ba–Pb oxide $Ba_{0.375}Pb_{0.625}Bi_2Nb_2O_9$ is orthorhombic in $A2_1am$ at room temperature and increasing the temperature results in a transition firstly to a paraelectric $Amam$ orthorhombic phase and ultimately to a tetragonal $I4/mmm$ structure. The transition between the two orthorhombic phases is accompanied by a dramatic change in the tilting of the NbO_6 octahedra. Increasing the Ba content reduces the degree of the orthorhombic distortion and it was anticipated from x-ray measurements that $Ba_{0.625}Pb_{0.375}Bi_2Nb_2O_9$ would be tetragonal at room temperature and would thus provide a test for the proposed sequence of transitions observed in the $BaBi_2Nb_2O_9$–$PbBi_2Nb_2O_9$ system. Clearly, higher Ba contents are required to stabilize the tetragonal structure at room temperature and examination of such complexes remains a high priority.

Acknowledgments

BJK acknowledges the support of the Australian Research Council. We are grateful to KEK for the provision of the neutron diffraction facilities for this work.

References

[1] Scott J F, Araujo C A, Meadows H B, McMillan L D and Shawabkeh A 1989 *J. Appl. Phys.* **66** 1444–53
[2] Larsen P K, Cuppens R and Spierings G A C M 1992 *Ferroelectrics* **128** 265–92
[3] de Araujo C A P, Cuchiaro J D, McMillan L D, Scott M C and Scott J F 1995 *Nature* **374** 627–9
[4] Ismunandar, Kennedy B J and Hunter B A 1998 *Solid State Ion.* **112** 281–9
[5] Macquart R, Kennedy B J and Shimakawa Y 2001 *J. Solid State Chem.* **160** 174–7
[6] Blake S M, Falconer M J, McCreedy M and Lightfoot P 1997 *J. Mater. Chem.* **7** 1609–13
[7] Kennedy B J and Hunter B A 2001 *Chem. Mater.* **13** 4612–7
[8] Macquart R, Kennedy B J, Hunter B A, Howard C J and Shimakawa Y 2002 *Integrated Ferroelectrics* **44** 101–12
[9] Stachiotti M G, Rodriguez C O, Ambrosch-Draxl C and Christensen N E 2000 *Phys. Rev.* B **61** 14434–9
[10] Miranda C, Costa M E V, Avdeev M, Kholkin A L and Baptista J L 2001 *J. Eur. Ceram. Soc.* **21** 1303–6
[11] Smolenskii G A, Isupov V A and Agranovskaya A I 1961 *Sov. Phys.—Solid State* **3** 651–5
[12] Shimakawa Y, Kubo Y, Nakagawa Y, Goto S, Kamiyama T, Asano H and Izumi F 2000 *Phys. Rev.* B **61** 6559–64
[13] Macquart R, Kennedy B J, Vogt T and Howard C J 2002 *Phys. Rev.* B **66** 2121021–4
[14] Park B H, Kang B S, Bu S D, Noh T W, Lee J and Jo W 1999 *Nature* **401** 682–4
[15] Chon U, Jang H M, Kim M G and Chang C H 2002 *Phys. Rev. Lett.* **89** 087601-1–4
[16] Garg A, Barber Z H, Dawber M, Scott J F, Snedden A and Lightfoot P 2003 *Appl. Phys. Lett.* **83** 2414–6
[17] Kamiyama T, Torii S, Mori K, Oikawa K, Itoh S, Furusaka M, Satoh S, Egami T, Izumi F and Asano H 2000 *Mater. Sci. Forum* **321–324** 302–7
[18] Hunter B A and Howard C J 1997 *Rietica. A Computer Program for Rietveld Analysis of X-ray and Neutron Powder Diffraction Patterns* (New South Wales: Lucas Heights Research Laboratories)
[19] Macquart R, Kennedy B J, Hunter B A and Howard C J 2002 *J. Phys.: Condens. Matter* **14** 7955–62
[20] Stokes H T and Hatch D M 1998 *Isotropy* (Uttah: Brigham Young University)
[21] Hervoches C H, Irvine J T S and Lightfoot P 2001 *Phys. Rev.* B **64** 100102-1–4
[22] Subbarao E C 1962 *J. Phys. Chem. Solids* **23** 665–76